

# Upregulated inflammatory associated factors and blood-retinal barrier changes in the retina of type 2 diabetes mellitus model

Rui-Jin Ran<sup>1,2</sup>, Xiao-Ying Zheng<sup>1</sup>, Li-Ping Du<sup>1</sup>, Xue-Dong Zhang<sup>1</sup>, Xiao-Li Chen<sup>1</sup>, Shen-Yin Zhu<sup>1</sup>

<sup>1</sup>Department of Ophthalmology, the First Affiliated Hospital of Chongqing Medical University, Chongqing Key Laboratory of Ophthalmology, Chongqing Eye Institute, Chongqing 400016, China

<sup>2</sup>University Hospital of Hubei University for Nationalities, Enshi 445000, Hubei Province, China

**Correspondence to:** Xue-Dong Zhang. Department of Ophthalmology, the First Affiliated Hospital of Chongqing Medical University, No.1 You Yi Road, Yu Zhong District, Chongqing 400016, China. zxued@sina.com

Received: 2015-05-06 Accepted: 2016-06-16

## Abstract

• **AIM:** To examine the expression of high mobility group box-1 (HMGB-1) and intercellular adhesion molecule-1 (ICAM-1) in the retina and the hippocampal tissues; and further to evaluate the association of these two molecules with the alterations of blood-retinal barrier (BRB) and blood-brain barrier (BBB) in a rat model of type 2 diabetes.

• **METHODS:** The type-2 diabetes mellitus (DM) model was established with a high-fat and high-glucose diet combined with streptozotocin (STZ). Sixteen weeks after DM induction, morphological changes of retina and hippocampus were observed with hematoxylin-eosin staining, and alternations of BRB and BBB permeability were measured using Evans blue method. Levels of HMGB-1 and ICAM-1 in retina and hippocampus were detected by Western blot. Serum HMGB-1 levels were determined by enzyme-linked immunosorbent assay (ELISA).

• **RESULTS:** A significantly higher serum fasting blood glucose level in DM rats was observed 2wk after STZ injection ( $P < 0.01$ ). The serum levels of fasting insulin, Insulin resistance homeostatic model assessment ( $IR_{HOMA}$ ), total cholesterol (TC), total triglycerides (TG) and low density lipoprotein cholesterol (LDL-C) in the DM rats significantly higher than those in the controls (all  $P < 0.01$ ). HMGB-1 ( $0.96 \pm 0.03$ ,  $P < 0.01$ ) and ICAM-1 ( $0.76 \pm 0.12$ ,  $P < 0.05$ ) levels in the retina in the DM rats were significantly higher than those in the controls. HMGB-1 ( $0.83 \pm 0.13$ ,  $P < 0.01$ ) and ICAM-1 ( $1.15 \pm 0.08$ ,  $P < 0.01$ ) levels in the hippocampal tissues in the DM rats were also

significantly higher than those in the controls. Sixteen weeks after induction of DM, the BRB permeability to albumin-bound Evans blue dye in the DM rats was significantly higher than that in the controls ( $P < 0.01$ ). However, there was no difference of BBB permeability between the DM rats and controls. When compared to the controls, hematoxylin and eosin staining showed obvious irregularities in the DM rats.

• **CONCLUSION:** BRB permeability increases significantly in rats with type-2 DM, which may be associated with the up-regulated retinal expression of HMGB-1 and ICAM-1.

• **KEYWORDS:** blood-retinal barrier; blood-brain barrier; diabetes mellitus; permeability; high mobility group box-1 protein; rats

**DOI:10.18240/ijo.2016.11.09**

Ran RJ, Zheng XY, Du LP, Zhang XD, Chen XL, Zhu SY. Upregulated inflammatory associated factors and blood-retinal barrier changes in the retina of type 2 diabetes mellitus model. *Int J Ophthalmol* 2016;9(11):1591-1597

## INTRODUCTION

The prevalence of type 2 diabetes mellitus (DM) is boosting in recent years, which stands as a heavy economic burden for the whole society. Macro- and micro-vasculopathy are the most common and serious complications of DM [1]. The latter, including diabetic retinopathy and encephalopathy, can lead to the visual acuity and cognition ability in patients with DM, respectively. The most fundamental aspect of blood-retinal barrier (BRB) and blood-brain barrier (BBB) is the barrier function, impeding various harmful substances from entering in. Furthermore, growing evidence has suggested that the disruptions of BRB and BBB are its early hallmarks [2-3] and foretell the subsequent retinal edema and central nervous system dysfunction, respectively. Recently, studies have suggested that certain pathologic conditions disrupting the integrity of BBB might concomitantly affect BRB due to the anatomical and functional similarity between them [2-3]. Though the exact mechanisms of diabetic micro-vasculopathy remain unclear, we hypothesized that diabetic retinopathy and encephalopathy may share certain same pathogenesis, including inflammation, which has been widely accepted as a

central part in the process of barrier breakdown [4-5]. High mobility group box-1 (HMGB-1), a multifunctional and nonhistone chromatin-binding protein, mainly presents in the nucleus where it can stabilize nucleosome formation and facilitate transcription. Extracellular HMGB-1, released by necrotic cells and injured tissues, was implicated as a mediator of both infectious and non-infectious inflammatory diseases [6]. Studies indicated that HMGB-1 could act as a proinflammatory cytokine and participate in various diabetic complications including retinopathy, cardiomyopathy and nephropathy [7-9]. More recently, HMGB-1 was reported to be involved in the pathogenesis of diabetic retinopathy via activation of inflammatory cascades [10]. Furthermore, retinal upregulation of HMGB-1 was demonstrated to participate in retinopathy by increasing BRB permeability in the rat model of streptozotocin (STZ)-induced DM, possibly through the production of various proinflammatory cytokines. As reported, intravitreal administration of HMGB-1 increased the permeability of BRB and protein expression of intercellular adhesion molecule-1 (ICAM-1) in the retinas of wild-type normal rats [11]. ICAM-1 mainly mediates the interaction between leukocytes and capillary endothelia as a proinflammatory cytokine, and enhanced expression of ICAM-1 is correlated to leukostasis [12]. Leukostasis within the retinal or cerebral vasculature may take a crucial role in BRB or BBB breakdown [13]. Noteworthy, blockage of ICAM-1 with neutralizing antibodies prevented leukocyte adhesion and hereby maintained the BRB [14]. In addition, increased BBB permeability was proved to be associated with the up-regulation of HMGB-1 in the hippocampus of rats with splenectomy surgery or with cerebral ischemia and reperfusion, in which circumstances inflammation was believed to take a part [15-16].

Over 90% of humans with DM are type 2, which develops due to insufficient insulin secretion and increased insulin resistance [17]. However, as far as we know, most basic studies about BRB or BBB were performed on insulinopenic (STZ-induced DM) model, which usually are used for type 1 DM. It is still known about the BRB/BBB in type 2 DM. Therefore, the present study aimed to reveal the alterations of BRB/BBB permeability and of HMGB-1/ICAM-1 expression in rats with type 2 DM.

## **MATERIALS AND METHODS**

**Animals** A total of 42 healthy male SD rats of 8-10wk old, weighed between 200 and 250 g, were used in this study. All rats were obtained from the Experimental Animal Center of Chongqing Medical University, where rats were housed in cages on a 12h light-dark schedule. All experiments were conducted in accordance with the international guidelines Principles of Laboratory Animals Care and were approved by the Animal Care Committee of Chongqing Medical University.

**Induction of Type 2 Diabetes Mellitus** After one week of adaptive feeding, rats were randomly and evenly assigned to two groups, normal control and DM group. Rats in the normal control group were fed with the laboratory regular diet, while rats in the DM group with a high-fat and high-glucose diet (10.0% lard, 20.0% sucrose, 2.5% cholesterol, and 67.5% regular diet), which may help to induce peripheral insulin resistance. Two weeks later, rats in the DM group were given an intraperitoneal injection of low-dose STZ (30 mg/kg) to induce type 2 DM by partially impairing insulin production. Meanwhile, rats served as the normal controls were subjected to intraperitoneal injection of an equivalent amount of citrate buffer (pH 4.5) alone. Blood glucose level greater than 16.7 mmol/L was taken as the criterion for successful establishment of DM model at 72h after STZ injection [18-19]. Maintenance of the diabetic state was confirmed by the measurements of tail vein blood glucose weekly. Rats failed to fit those requirements were excluded from our study together with the dead ones. Ultimately, 19 rats were included in the normal control group and 17 in the DM group. Sixteen weeks after successful DM induction, animals were sacrificed for further experiments.

**Biochemical Measurements** Body weight (BW) was measured with an electronic balance. Fasting insulin (FINS) was determined by a rat antibody radioimmunoassay (Linco Diagnostics, St. Charles, MO, USA) with an automated radioimmunoassay instrument (USTC Chuangxin Co., Ltd. Zonkia Branch, Anhui Province, China). Fasting blood glucose (FBG) was evaluated with the hexokinase assay using the automatic biochemical analyzer (model AU2700, Olympus Diagnostics, Holliston, MA, USA). Measurements of total cholesterol (TC), total triglycerides (TG) and low density lipoprotein cholesterol (LDL-C) were performed using the lipase method with the same biochemical analyzer. Insulin resistance (IR) was calculated using the homeostatic model assessment (HOMA) equation:  $IR_{HOMA} = FINS \times FBG / 22.5$ .

**Enzyme-linked Immunosorbent Assay** All rats were anaesthetized with 100 g/L hydral (3-4 mL/kg BW) administered subcutaneously, followed by cardiac puncture for blood withdrawal. Blood samples were centrifuged at 3000 rpm for 15min and the serum supernatants were separated, aliquoted, and immediately stored at -80°C. One part of the blood sample was used for assessment of biochemical parameters as described above. And the remaining portion for evaluation of HMGB-1 protein level with a rat antibody commercial enzyme-linked immunosorbent assay (ELISA) kit (Shino-Test Corporation, Tokyo, Japan), according to the manufacturer's instructions. The absorbance at 450 nm was determined by an automated plate reader (Spectra Max Gemini UVmax; Molecular Devices, Sunnyvale, CA, USA). All measurements were performed in triplicate.

**Hematoxylin and Eosin Staining** The eyeballs and hippocampus separated from brains were subjected to 4% paraformaldehyde solution at 4°C overnight. Those eyeballs with anterior segments removal and hippocampus were then dehydrated transparentized and embedded in paraffin blocks. Sections of four to five micron thickness were cut and transferred to triethoxysilane-coated slides. After being dewaxed and washed thoroughly, these sections were stained with hematoxylin-eosin (HE), followed by being dehydrated and cemented with neutral resins. Then, the histopathological abnormalities were investigated under a light microscope, and photographs were taken with an Olympus BX60 microscope (Olympus Optical Co. Ltd., Tokyo, Japan).

**Rat Blood-retinal Barrier and Blood-brain Barrier Breakdown Measurement** The permeability of BRB and BBB were determined using the Evans blue (EB) method as previously described with minor modifications<sup>[20-21]</sup>. EB dye is known to bind to serum albumin after intravenous injection and therefore could be used as a tracer for serum albumin. Briefly, after the rats were deeply anesthetized, EB dye (30 mg/mL in saline, 45 mg/kg BW) was injected into the femoral vein. The rats were kept on a warm pad to ensure the complete circulation of the dye. One hour after dye injection, the chest cavity was opened and the left ventricle was cannulated. Then, 0.2 mL of total blood was obtained and centrifuged at 12 000 rpm for 15min. Each rat was perfused with saline containing 1% paraformaldehyde (37°C, contained 10 IU/mL heparin) at 110 mm Hg pressure for 15min until the fluid from the right atrium became colorless. After decapitation, the eyes were removed immediately and retinas were dissected carefully. In addition, the brain was removed and hippocampus was procured particularly. Then, the retinal and hippocampal tissues were weighed and homogenized separately in formamide (4:1, volume/weight). The homogenate was incubated for 24h at 60°C and centrifuged at 12 000 rpm for 45min at 4°C to obtain supernatant. Afterwards the supernatant was measured at 620 nm (absorbance maximum for EB in formamide) and 740 nm (absorbance minimum) using a spectrophotometer. The concentration of EB in retinal and hippocampal tissues was calculated from their respective standard curves, and the breakdown of BRB and BBB was calculated accordingly.

**Western Blot Analysis** Retinas were isolated and sonicated in RIPA buffer [20 mmol/L Tris-HCl, pH 7.5, 150 mmol/L NaCl, 5 mmol/L EDTA, 1 mmol/L Na<sub>3</sub>VO<sub>4</sub>, 1 mmol/L phenylmethylsulfonyl fluoride (PMSF), 20 µg/mL aprotinin, 20 µg/mL leupeptin, and 1% NP-40] for 5min. Hippocampal tissues were homogenized in the same lysis buffer for 30min. Retinal and hippocampal lysates were centrifuged at 12 000 rpm for 20min at 4°C and the supernatants were collected respectively. Protein concentrations were determined using the Bio-Rad method (Bio-Rad, Richmond,

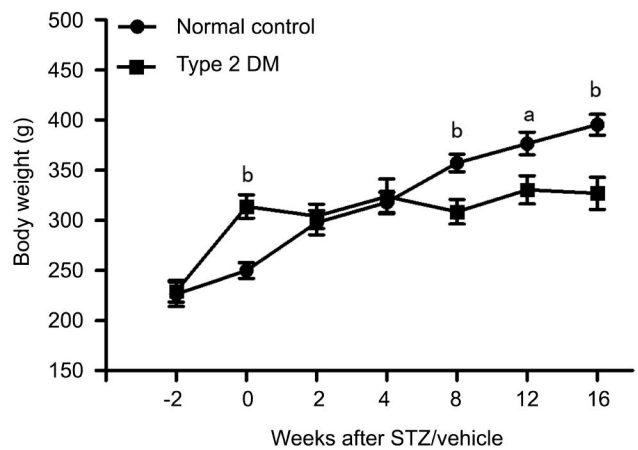


**Figure 1** BW of rats with type 2 DM and normal controls BW (g) was measured at weekly intervals starting at 2wk prior to STZ/vehicle injection to the end of the study period. Data are mean±SD (*n* =8 per group). STZ: Streptozotocin; DM: Diabetes mellitus. <sup>a</sup>*P*<0.05 *vs* normal control; <sup>b</sup>*P*<0.01 *vs* normal control.

CA, USA). For immunoblotting, equal amounts of protein per lane were loaded and electrophoresed on 10% polyacrylamide gels, and then transferred to polyvinylidene fluoride (PVDF) membranes. The membranes were blocked with 5% nonfat milk for 2h, followed by incubation with anti-HMGB-1 antibody (1:500, Epitomics, Cambridge, UK), anti-ICAM-1 antibody (1:500, Abcam, Cambridge, UK) or anti-actin antibody (1:1000, Sigma, St. Louis, MO, USA) at 4°C overnight. Then, the membranes were rinsed three times with TBST buffer (150 mmol/L NaCl, 10 mmol/L Tris-HCl, and 0.1% Tween 20) and incubated with secondary horseradish peroxidase-conjugated antibody (Abcam, Cambridge, UK) for 1h at 37°C. The immunocomplexes were visualized by the enhanced chemiluminescence (ECL) chemiluminescence method. Subsequently, protein bands were quantified with the densitometry analysis (quantity one software).

**Statistical Analysis** All data were expressed as mean ± standard deviation (SD) unless otherwise specified. The statistical analysis was determined by an unpaired and two-tailed Student's *t*-test using GraphPad Prism software (version 4.0, GraphPad Software, San Diego, Calif, USA). *P* value less than 0.05 was considered statistically significant.

## RESULTS

**General Characteristics of Rats** During the observation period, rat BWs were shown in Figure 1. At the time of STZ/vehicle injection, rats fed with a high-fat and high-glucose diet for the prior 2wk were heavier (314±42 g) than those with the regular rat chow (250±28 g). Rats in the normal control group continued to gain weight throughout the study period; however, rats in the type 2 DM group had regained their pre-STZ injection weights at the time of sacrifice (327±58 g). Rats with type 2 DM were listless and unresponsive in general. They had dull and tarnished coats,

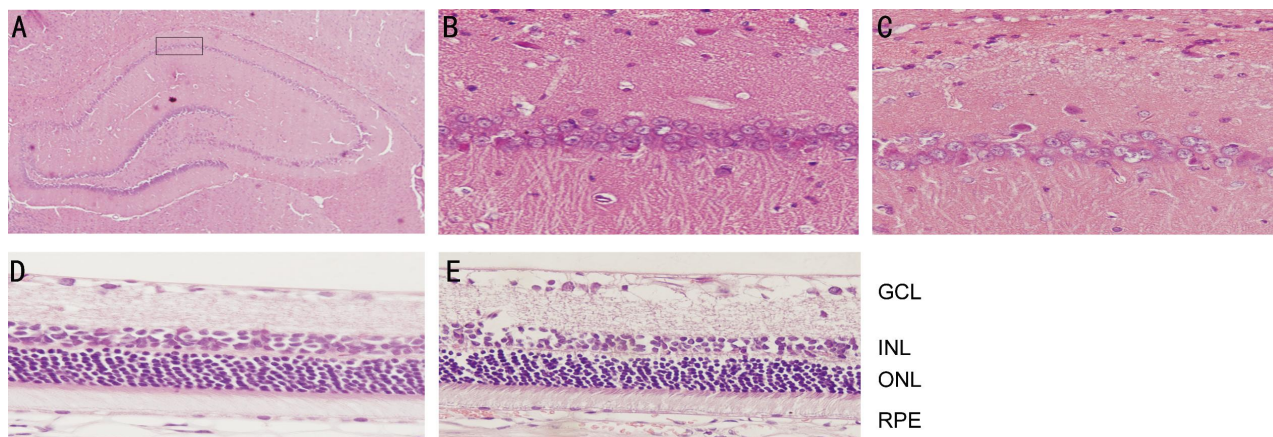


**Figure 2 Representative images of hippocampal and retinal tissues with HE staining** A: The CA1 region of rat hippocampus used for study; B: Hippocampal tissue in the normal control group: no obvious histopathological abnormalities were found; C: Hippocampal tissue in the type 2 DM group: the pyramidal cells appeared decreased in quantity and were arranged irregularly; D: Retinal tissue in the normal control group: the shape of retinal cells in each layer was normal and these cells were lined up orderly; E: Retinal tissue in the type 2 DM group: the edema of retinal GCL, thickening of inner plexiform layer and disordered arrangement of INL. Original magnification was 400× except that the magnification in A was 100×. GCL: Ganglion cell layer; INL: Inner nuclear layer; ONL: Outer nuclear layer; RPE: Retinal pigment epithelium layer.

**Table 1 Serum chemistry levels of rats in the normal control and type 2 DM groups** *n*=8 per group,  $\bar{x} \pm s$

Parameters	Before STZ/vehicle		2wk after STZ/vehicle	
	Normal control	Type 2 DM	Normal control	Type 2 DM
FBG (mmol/L)	5.48±0.80	5.61±0.50	5.69±0.78	18.86±5.22 <sup>b</sup>
FINS (IU/mL)	13.08±3.79	53.68±6.14 <sup>b</sup>	13.53±3.41	43.32±10.81 <sup>b</sup>
IR <sub>HOMA</sub>	3.12±0.78	13.31±1.37 <sup>b</sup>	3.39±0.88	38.65±16.33 <sup>b</sup>
TC (mmol/L)	1.22±0.18	2.44±0.23 <sup>b</sup>	1.46±0.14	3.84±0.42 <sup>b</sup>
TG (mmol/L)	0.42±0.15	0.86±0.32 <sup>b</sup>	0.43±0.17	1.82±0.77 <sup>b</sup>
LDL-C (mmol/L)	0.41±0.05	1.09±0.11 <sup>b</sup>	0.38±0.06	1.58±0.14 <sup>b</sup>

FBG: Fasting blood glucose; FINS: Fasting insulin; IR<sub>HOMA</sub>: Insulin resistance homeostatic model assessment; TC: Total cholesterol; TG: Total triglycerides; LDL-C: Low density lipoprotein cholesterol; STZ: Streptozotocin; DM: Diabetes mellitus. <sup>b</sup>*P*<0.01 vs normal control.

also developed typical manifestations of DM such as polydipsia, polyphagia and polyuria. In contrast, rats in the normal control group were active and responsive, and had shiny and soft coats.

**Serum Biochemical Parameters and Insulin Resistance Index** As shown in Table 1, before STZ injection, there was no difference of serum FBG levels between the rats fed with high-fat diet and the normal controls. Two weeks after STZ injection, there was a significant increase of serum FBG levels in the type 2 DM group when compared with that in the normal controls (*P*<0.01). The serum levels of FINS, IR<sub>HOMA</sub>, TC, TG, and LDL-C of rats in the type 2 DM group were significantly higher than those of rats in the normal control group (all *P*<0.01) at the time of as well as 2wk after STZ/vehicle injection.

**Pathomorphology Observation of the Hippocampal and Retinal Tissues** HE staining showed no obvious neural irregularities in the hippocampal tissues of rats in the normal control group. The pyramidal cells, round and intact with nuclei stained dark blue, were arranged tightly and neatly in the cornu ammonis 1 (CA1) region (Figure 2B). However,

rats with type 2 DM showed obvious hippocampal histopathological damage. The pyramidal layered structure was distorted in the CA1 region and the number of cells appeared decreased when compared with controls (Figure 2C). Meanwhile, HE staining revealed no remarkable retinal abnormalities in the normal control group, as retinal cells were well-shaped and aligned organically in each layer of retinal tissues (Figure 2D). There was a presence of edema in the retinal ganglion cell layer, thickening of inner plexiform layer, and disordered arrangement of inner nuclear layer in the type 2 DM group (Figure 2E).

**Alterations of Blood-retinal Barrier and Blood-brain Barrier Permeability in Rats with Type 2 DM** Sixteen weeks after the injection of STZ, the BRB permeability to albumin-bound EB dye significantly increased in rats with type 2 DM when compared with that in the normal controls (*P*<0.01) (Figure 3A). Unexpectedly, the BBB permeability assessed by EB method only slightly upregulated in the type 2 DM group when compared with that in the normal controls, failing to reach a statistic difference (Figure 3B).

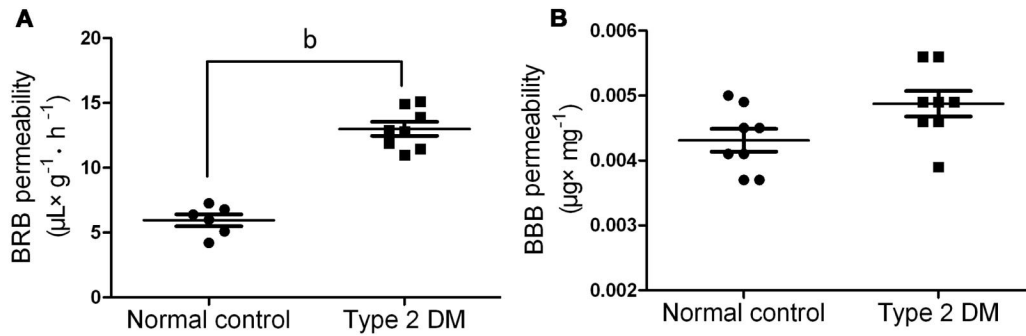


**Figure 3 Permeability of BRB and BBB in the normal control and type 2 DM rats** A: BRB permeability, data are presented as  $\mu\text{L}$  plasma  $\times$  g retina wet weight $^{-1}$  hour $^{-1}$  and represent the mean $\pm$ SD of 6-8 rats. <sup>b</sup> $P < 0.01$  vs normal control; B: BBB permeability, data are presented as  $\mu\text{g}$  of EB per wet weight (mg) of hippocampus and represent the mean $\pm$ SD of 8 rats. The permeability of BRB and BBB was estimated by quantification of extravasated EB as described in Methods. No significant difference was found between the normal control and type 2 DM group.

**Protein Expression of High Mobility Group Box-1 and Intercellular Adhesion Molecule -1 in Retinal and Hippocampal Tissues**

Protein expression of HMGB-1 and ICAM-1 was evaluated by Western blot. The retinal tissues of rats with type 2 DM showed significantly enhanced protein expression of HMGB-1 ( $0.96 \pm 0.03$ ,  $P < 0.01$ ) and ICAM-1 ( $0.76 \pm 0.12$ ,  $P < 0.05$ ), when compared with the normal controls (Figure 4). Similarly, rats with type 2 DM demonstrated a significantly higher protein expression of HMGB-1 ( $0.83 \pm 0.13$ ,  $P < 0.01$ ) and ICAM-1 ( $1.15 \pm 0.08$ ,  $P < 0.01$ ) in the hippocampal tissues, when compared with the normal controls.

**Protein Expression of High Mobility Group Box-1 in the Serum** The levels of serum HMGB-1 in the rats were determined by ELISA. There was no difference in serum HMGB-1 levels between the type 2 DM and normal control group, though HMGB-1 levels appeared a little higher in the type 2 DM group ( $1.19 \pm 0.14$  vs  $1.04 \pm 0.18$  ng/mL,  $P = 0.303$ ,  $n = 5-8$ ).

**DISCUSSION**

Though the pathogenesis of micro-vasculopathy, the most common complication of DM, is still unknown, the breakdown of BRB and BBB has been considered as the prodromal lesions of micro-vasculopathy in the retina and brain. The present study showed that BRB permeability together with retinal expression of HMGB-1 and ICAM-1 was increased in rats with type 2 DM, when compared to the normal controls. Surprisingly, there was no difference of BBB permeability (hippocampus) between the DM rats and the normal controls, although hippocampal expression of HMGB-1 and ICAM-1 were strengthened in the type 2 DM rats.

In Mohammad *et al*'s [11] study on rats with STZ-induced DM, BRB permeability increased significantly in rats with type 2 DM compared with the normal controls, which was confirmed in our present study. However, there was no difference in the BBB permeability (hippocampus) between

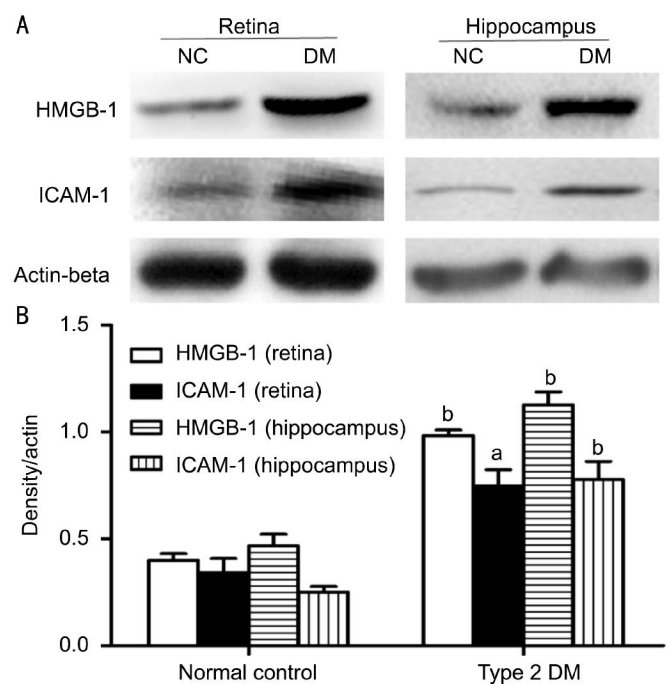


**Figure 4 Protein expression of HMGB-1 and ICAM-1 in rat retina and hippocampus** A: Representative Western blot showing the protein expression of HMGB-1 and ICAM-1 in rat retina and hippocampus. Equal amounts of proteins were loaded and Actin-beta was used as a loading control,  $n = 4$  experiments; B: Column diagrams and bars representing the ratio of the scanned immunoblots of HMGB-1 and ICAM-1 to that of Actin-beta. Data are shown as mean $\pm$ SD,  $n = 4$  experiments, <sup>a</sup> $P < 0.05$  vs normal control, <sup>b</sup> $P < 0.01$  vs normal control.

type 2 DM and normal control group at the end of our experiment period (16wk). This finding was in consistent with evidence presented by Karolczak *et al* [22], showing that no significant difference was observed in EB fluorescence in hippocampus between STZ-induced diabetic and normal control rats. But Huber *et al* [23] reported that STZ-induced DM caused a progressive increase in BBB permeability to the whole brain and ultimately hippocampal BBB was compromised in rats at 90d. The discrepancy between Huber *et al*'s [23] study and ours may be ascribed to the different

types of DM model used for experiments. Since DM-induced BBB damage was region specific to the brain, it is rational to speculate that hippocampal BBB remained preserved at 16wk duration of type 2 DM but not of STZ-induced DM.

Increased BRB permeability is a hallmark of early diabetic retinopathy, and the pathogenesis of BRB breakdown is intricate and has not been fully unveiled so far. Recently, HMGB-1 signaling pathway components were found to be up-regulated in the retinas of rats with STZ-induced DM, and exogenous HMGB-1 was reported to induce BRB breakdown *via* enhancing the production of ICAM-1 in non-diabetic normal rodents [11]. ICAM-1 is a well-known and important inflammatory adhesion molecule involved in leukocyte-endothelial cell interaction, which results in the damage of endothelial cell function and subsequently increases vascular permeability [24-25]. To our expectation, our study showed that retinal protein expression of HMGB-1 and ICAM-1 was upregulated, which may be correlated to the BRB breakdown in rats with type 2 DM. However, protein levels of serum HMGB-1 were not significantly different between type 2 DM and normal control group. Since Yan *et al* [26] reported that elevated production of serum HMGB-1 was associated with coronary artery disease in patients with type 2 DM, we considered that the small sample size in our study might be counted as the reason for the discrepancy.

Unexpectedly, in our experiment, the BBB permeability of hippocampus showed no significant difference between diabetic and normal control rats, although protein expression of HMGB-1 and ICAM-1 in hippocampus was elevated significantly in rats with type 2 DM. There may be three reasons for this inconsistency. Firstly, since increased HMGB-1 was confirmed to be closely associated with the BBB breakdown in many cerebral diseases [27-28], we assumed that the BBB permeability of other cerebral regions like midbrain, but not of hippocampus, probably increased along with the up-regulation of HMGB-1. Secondly, while 16wk were long enough to up-regulate the hippocampal expression of HMGB-1 and ICAM-1, it may not be adequate to develop manifest hippocampal BBB breakdown in rats with type 2 DM. Lastly, the EB method for measurement of BBB permeability might not be sensitive enough to detect its alternations in the early stage of diabetic encephalopathy, other assays may be used as alternatives [29]. However, the exact mechanisms need further elucidation.

Limitation of the present study is that we could not block the HMGB-1 and ICAM-1. And the precise role of up-regulated HMGB-1 and ICAM-1 in the development of BRB is just a reasonable speculation based on related studies published previously. Further studies are needed to confirm the association [11,24-25]. Secondly, the present studies did not demonstrate the reasons for the discrepancy of between the DM retinopathy and encephalopathy.

Taken together, the present study demonstrated that the permeability of BRB but not of hippocampal BBB was increased significantly in rats subjected to experimental model of type 2 DM. The increased permeability of BRB in DM rats may be associated with the up-regulation of HMGB-1 and ICAM-1 in retinas. These results may shed new light on the mechanisms involved in the micro-vasculopathy caused by diabetic retinopathy, though the precise mechanisms need further clarification.

#### ACKNOWLEDGEMENTS

**Foundation:** Supported by the Project of Education Bureau Foundation of Hubei Province (No. Q20151901).

**Conflicts of Interest:** Ran RJ, None; Zheng XY, None; Du LP, None; Zhang XD, None; Chen XL, None; Zhu SY, None.

#### REFERENCES

- Xu Y, Wang L, He J, Bi Y, Li M, Wang T, Wang L, Jiang Y, Dai M, Lu J, Xu M, Li Y, Hu N, Li J, Mi S, Chen CS, Li G, Mu Y, Zhao J, Kong L, Chen J, Lai S, Wang W, Zhao W, Ning G; 2010 China Noncommunicable Disease Surveillance Group. Prevalence and control of diabetes in Chinese adults. *JAMA* 2013;310(9):948-959.
- Greiner J, Dorovini-Zis K, Taylor TE, Molyneux ME, Beare NA, Kamiza S, White VA. Correlation of hemorrhage, axonal damage, and blood-tissue barrier disruption in brain and retina of Malawian children with fatal cerebral malaria. *Front Cell Infect Microbiol* 2015;5:18.
- Ozkan E, Gocmen R, Topcuoglu MA, Arsava EM. Blood-retina-barrier disruption accompanying blood-brain-barrier dysfunction in posterior reversible encephalopathy syndrome. *J Neurol Sci* 2014;346 (1-2): 315-317.
- van den Berg E, Reijmer YD, de Bresser J, Kessels RP, Kappelle LJ, Biessels GJ; Utrecht Diabetic Encephalopathy Study Group. A 4 year follow-up study of cognitive functioning in patients with type 2 diabetes mellitus. *Diabetologia* 2010;53(1):58-65.
- Forster C. Tight junctions and the modulation of barrier function in disease. *Histochem Cell Biol* 2008;130(1):55-70.
- Voll RE, Urbonaviciute V, Herrmann M, Kalden JR. High mobility group box 1 in the pathogenesis of inflammatory and autoimmune diseases. *Isr Med Assoc J* 2008;10(1):26-28.
- Volz HC, Seidel C, Laohachewin D, Kaya Z, Müller OJ, Pleger ST, Lasitschka F, Bianchi ME, Remppis A, Bierhaus A, Katus HA, Andrassy M. HMGB1: the missing link between diabetes mellitus and heart failure. *Basic Res Cardiol* 2010;105(6):805-820.
- Nogueira-Machado JA, Volpe CM, Veloso CA, Chaves MM. HMGB1, TLR and RAGE: a functional tripod that leads to diabetic inflammation. *Expert Opin Ther Targets* 2011;15(8):1023-1035.
- Kim J, Sohn E, Kim CS, Jo K, Kim JS. The role of high-mobility group box-1 protein in the development of diabetic nephropathy. *Am J Nephrol* 2011;33(6):524-529.
- El-Asrar AM. Role of inflammation in the pathogenesis of diabetic retinopathy. *Middle East Afr J Ophthalmol* 2012;19(1):70-74.
- Mohammad G, Siddiquei MM, Othman A, Al-Shabrawey M, Abu El-Asrar AM. High-mobility group box-1 protein activates inflammatory signaling pathway components and disrupts retinal vascular-barrier in the diabetic retina. *Exp Eye Res* 2013;107:101-109.
- Pazdrak K, Young TW, Stafford S, Olszewska-Pazdrak B, Straub C, Starosta V, Brasier A, Kurosky A. Cross-talk between ICAM-1 and granulocyte-macrophage colony-stimulating factor receptor signaling

- modulates eosinophil survival and activation. *J Immunol* 2008;180 (6): 4182-4190.
- 13 Jousseaume AM, Poulaki V, Le ML, Koizumi K, Esser C, Janicki H, Schraermeyer U, Kociok N, Fauser S, Kirchhof B, Kern TS, Adamis AP. A central role for inflammation in the pathogenesis of diabetic retinopathy. *FASEB J* 2004;18(12):1450-1452.
- 14 Miyamoto K, Khosrof S, Bursell SE, Moromizato Y, Aiello LP, Ogura Y, Adamis AP. Vascular endothelial growth factor (VEGF)-induced retinal vascular permeability is mediated by intercellular adhesion molecule-1 (ICAM-1). *Am J Pathol* 2000;156(5):1733-1739.
- 15 Luan H, Kan Z, Xu Y, Lv C, Jiang W. Rosmarinic acid protects against experimental diabetes with cerebral ischemia: relation to inflammation response. *J Neuroinflammation* 2013;10:28.
- 16 He HJ, Wang Y, Le Y, Duan KM, Yan XB, Liao Q, Liao Y, Tong JB, Terrando N, Ouyang W. Surgery upregulates high mobility group box-1 and disrupts the blood-brain barrier causing cognitive dysfunction in aged rats. *CNS Neurosci Ther* 2012;18(12):994-1002.
- 17 Seto SW, Yang GY, Kiat H, Bensoussan A, Kwan YW, Chang D. Diabetes mellitus, cognitive impairment, and traditional Chinese medicine. *Int J Endocrinol* 2015;2015:810439.
- 18 Skovsø S. Modeling type 2 diabetes in rats using high fat diet and streptozotocin. *J Diabetes Investig* 2014;5(4):349-358.
- 19 Winzell MS, Ahrén B. The high-fat diet-fed mouse: a model for studying mechanisms and treatment of impaired glucose tolerance and type 2 diabetes. *Diabetes* 2004;53 suppl 3:S215-219.
- 20 Chen Y, Li F, Meng X, Li X. Suppression of retinal angiogenesis by quercetin in a rodent model of retinopathy of prematurity. *Zhonghua Yi Xue Za Zhi* 2015;95(14):1113-1115.
- 21 Xu Q, Qaum T, Adamis AP. Sensitive blood-retinal barrier breakdown quantitation using Evans blue. *Invest Ophthalmol Vis Sci* 2001;42 (3): 789-794.
- 22 Karolczak K, Rozalska S, Wieczorek M, Labieniec-Watala M, Watala C. Poly (amido)amine dendrimers generation 4.0 (PAMAM G4) reduce blood hyperglycaemia and restore impaired blood-brain barrier permeability in streptozotocin diabetes in rats. *Int J Pharm* 2012;436(1-2):508-518.
- 23 Huber JD, Van Gilder RL, Houser KA. Streptozotocin-induced diabetes progressively increases blood-brain barrier permeability in specific brain regions in rats. *Am J Physiol Heart Circ Physiol* 2006;291 (6):H2660-2668.
- 24 Kaji Y, Usui T, Ishida S, Yamashiro K, Moore TC, Moore J, Yamamoto Y, Yamamoto H, Adamis AP. Inhibition of diabetic leukostasis and blood-retinal barrier breakdown with a soluble form of a receptor for advanced glycation end products. *Invest Ophthalmol Vis Sci* 2007;48 (2): 858-865.
- 25 Miyamoto K, Khosrof S, Bursell SE, Rohan R, Murata T, Clermont AC, Aiello LP, Ogura Y, Adamis AP. Prevention of leukostasis and vascular leakage in streptozotocin-induced diabetic retinopathy via intercellular adhesion molecule-1 inhibition. *Proc Natl Acad Sci U S A* 1999;96(19): 10836-10841.
- 26 Yan XX, Lu L, Peng WH, Wang LJ, Zhang Q, Zhang RY, Chen QJ, Shen WF. Increased serum HMGB1 level is associated with coronary artery disease in nondiabetic and type 2 diabetic patients. *Atherosclerosis* 2009; 205(2):544-548.
- 27 Vezzani A, French J, Bartfai T, Baram TZ. The role of inflammation in epilepsy. *Nat Rev Neurol* 2011;7(1):31-40.
- 28 Okuma Y, Liu K, Wake H, Zhang J, Maruo T, Date I, Yoshino T, Ohtsuka A, Otani N, Tomura S, Shima K, Yamamoto Y, Yamamoto H, Takahashi HK, Mori S, Nishibori M. Anti-high mobility group box-1 antibody therapy for traumatic brain injury. *Ann Neurol* 2012;72 (3): 373-384.
- 29 Le Sueur LP, Collares-Buzato CB, da Cruz-Höfling MA. Mechanisms involved in the blood-brain barrier increased permeability induced by Phonetria nigriventer spider venom in rats. *Brain Res* 2004;1027 (1-2): 38-47.